

PAPER

## Quantum conductance and switching kinetics of AgI-based microcrossbar cells

To cite this article: S Tappertzhofen *et al* 2012 *Nanotechnology* **23** 145703

View the [article online](#) for updates and enhancements.

### You may also like

- [Uniform Recalibration of Common Spectrophotometry Standard Stars onto the CALSPEC System Using the SuperNova Integral Field Spectrograph](#)  
David Rubin, G. Aldering, P. Antilogus et al.
- [THE AFTERGLOW AND ENVIRONMENT OF THE SHORT GRB 111117A](#)  
R. Margutti, E. Berger, W. Fong et al.
- [RELATIVISTIC \( \$E > 0.6\$ ,  \$> 2.0\$ , AND  \$> 4.0\$  MeV\) ELECTRON ACCELERATION AT GEOSYNCHRONOUS ORBIT DURING HIGH-INTENSITY, LONG-DURATION, CONTINUOUS AE ACTIVITY \(HILDCAA\) EVENTS](#)  
Rajkumar Hajra, Bruce T. Tsurutani, Ezequiel Echer et al.



**ECS**  
The  
Electrochemical  
Society  
Advancing solid state &  
electrochemical science & technology

**DISCOVER**  
how sustainability  
intersects with  
electrochemistry & solid  
state science research

# Quantum conductance and switching kinetics of AgI-based microcrossbar cells

S Tappertzhofen<sup>1,2</sup>, I Valov<sup>1,2,3</sup> and R Waser<sup>1,2,3</sup>

<sup>1</sup> Institut für Werkstoffe der Elektrotechnik II, RWTH Aachen University, 52074 Aachen, Germany

<sup>2</sup> JARA-FIT, Fundamentals of Future Information Technology, 52425 Jülich, Germany

<sup>3</sup> Peter Grünberg Institut 7, Forschungszentrum Jülich GmbH, 52425 Jülich, Germany

E-mail: [i.valov@fz-juelich.de](mailto:i.valov@fz-juelich.de)

Received 16 January 2012, in final form 9 February 2012

Published 21 March 2012

Online at [stacks.iop.org/Nano/23/145703](http://stacks.iop.org/Nano/23/145703)

## Abstract

Microcrossbar structured electrochemical metallization (ECM) cells based on silver iodide (AgI) solid electrolyte were fabricated and analyzed in terms of the resistive switching effect. The switching behavior implies the existence of quantized conductance higher than  $78 \mu\text{S}$  which can be identified as a multiple of the single atomic point contact conductivity. The nonlinearity of the switching kinetics has been analyzed in detail. Fast switching in at least 50 ns was observed for short pulse measurements.

(Some figures may appear in colour only in the online journal)

## 1. Introduction

Resistive switching random access memory (ReRAM) cells are intensively studied due to the prospect of high scalability and low power consumption, being considered as the most promising candidate to replace flash-based nonvolatile memory devices [1, 2]. Recently, within the context of ReRAM electrochemical metallization cells attracted a great deal of attention due to their simple structure, ease of fabrication and potential multibit storage [3]. The ECM cell arrangement consists of an electrolyte material sandwiched between an electrochemically inert counter electrode (CE, e.g. platinum) and a working electrode (WE, e.g. silver). By applying voltage or current pulses the resistance of the cell can be reversibly modulated between a high resistive state (HRS) and a low resistive state (LRS), depending on the voltage polarity. Hereby, the electrochemical formation and rupture of a nanoscaled metallic filament is believed to be responsible for the resistance transition [3].

Typically, amorphous oxides (such as  $\text{SiO}_2$  [4],  $\text{TiO}_2$  [5] or  $\text{Ta}_2\text{O}_5$  [6]) or higher chalcogenides (such as  $\text{GeS}_x$  or  $\text{GeSe}_x$  [7–9]) are used as solid electrolytes. As deposited, these material systems are insulators and do not initially contain mobile metallic ions (e.g.  $\text{Ag}^+$ ) [3] which are required for ionic transport and the filament formation. Hence, to enable resistive switching, ions need to be first injected into the insulator [10] by thermal diffusion [11]

or by applying a voltage pulse (electroforming voltage) which is typically higher than the subsequent switching voltages [12]. However, for  $\text{GeSe}_x$  films it has been reported that Ag and Cu can be chemically dissolved and easily diffuse into the electrolyte, even without a heat treatment [9]. In contrast, silver halogenides such as (poly-) crystalline silver iodide (AgI) initially contain mobile  $\text{Ag}^+$  ions which makes AgI a promising candidate for fast resistive switching applications. In the past, resistive switching in pure AgI [13] and AgI-based electrolytes such as  $\text{AgI-Ag}_2\text{O-WO}_3$  [14] or  $(\text{AgI})_{0.5}(\text{AgPO}_3)_{0.5}$  [15] has been observed but not investigated in terms of switching kinetics, filament conductivity or multilevel switching in detail yet. In particular, pattern transfer of the electrolyte is challenging since AgI is rather sensitive towards many chemicals, temperature and electron beams as well as UV light which is used in most process steps for fabrication of highly dense integrated memory devices.

Furthermore, the very nature of the contact resistance of the filament and the working electrode of ECM cells is as yet unknown. Since adjusting the ON resistance by orders of magnitudes depending on the current compliance (multilevel switching) has been reported for many ECM systems [3], tunneling and metallic contacts are both discussed [16]. Terabe *et al* observed quantized conductance of a vacuum-gap-based (gap-type) ECM cell [17]. Lately, a comprehensive study on quantized resistances for a gap-type

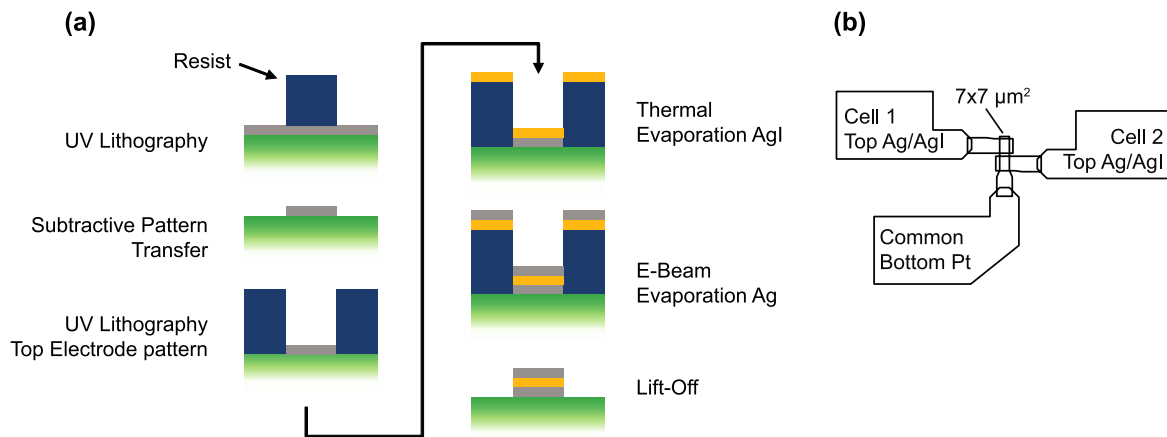


**Figure 1.** (a) Schematic presentation of the process steps for microcrossbars. (b) Layout of fabricated microcrossbars with a common Pt bottom electrode and two Ag/AgI top layers. For simplification, the SiO<sub>2</sub> and TiO<sub>2</sub> layers are not shown in the figure.

ECM system was done by Nayak *et al* [18]. They observed that the cell resistance is dominated by tunneling between filament and electrode for comparatively high resistances. Below 13 kΩ the resistance is dominated by atomic point contacts resulting in discrete resistance values depending on the particular number of atoms short-circuiting the filament and electrode. This behavior has yet not been studied for gapless ECM cells where the filament is growing within the solid electrolyte.

In this work we present a fabrication process for integrated AgI-based microcrossbar structured ECM cells. Low power resistive switching with currents down to 10 nA as well as multibit storage was observed by potentiodynamic current/voltage ( $I/V$ ) sweeps. We report on the conductivity mechanism of the filament short-circuiting the working and counter electrode. The switching kinetics of the ECM memory cells were analyzed by fast voltage pulses down to pulse lengths of 50 ns.

## 2. Experimental details

P-doped (100)-oriented silicon wafers were used as substrates to prepare microcrossbar structures. To improve the adhesion a 450 nm thick SiO<sub>2</sub> layer was fabricated by wet oxidation of the Si substrate followed by a 15 nm thick TiO<sub>2</sub> layer, deposited by DC magnetron sputtering of titanium and subsequent oxidation in a diffusion furnace. On this adhesion layer a 30 nm thick platinum bottom electrode was deposited by DC magnetron sputtering. A schema of the process steps for microcrossbar structured cells is shown in figure 1(a).

Based on this layer stack, the subtractive pattern transfer of the bottom electrode with overlapping electrode areas between 4 and 100 μm<sup>2</sup> was done using conventional UV lithography and reactive ion etching (RIE). The remaining photoresist was removed using the photoresist remover EKC 830 (DuPont Electronic Technologies) followed by an ultrasonic bath in acetone, isopropanol and deionized water for 10 min, respectively. To prevent the impact of UV light or alkaline-based resist developers on the AgI film, the top electrode pattern was prepared by UV lithography directly

after the bottom electrode was fabricated. Afterwards, a 30 nm thick AgI layer was deposited by thermal evaporation (0.5 nm s<sup>-1</sup>) in a high vacuum (10<sup>-5</sup> mbar). A 200 nm thick Ag top electrode was subsequently deposited by electron-beam (e-beam) evaporation. The sample fabrication was finally finished by a lift-off in acetone, isopropanol and deionized water for 5 min, respectively. Due to the mask layout two top electrodes sharing a common bottom electrode were fabricated simultaneously. Each top electrode is acting as an individual switching cell with the common bottom electrode. The layout is depicted in figure 1(b).

All measurements were performed at room temperature and ambient conditions in a dark chamber in order to avoid any impact of UV light. The crystal structure of the evaporated AgI films was analyzed by x-ray diffraction (XRD) using an X'Pert Pro diffractometer (PANalytical) in  $\Theta$ -2 $\Theta$  geometry equipped with an Anton Paar XRK 900 thermal processing chamber under ambient atmosphere. This equipment allows heating the sample at a constant rate of 4 °C min<sup>-1</sup> while simultaneously monitoring crystalline responses. The peak positions of the XRD diffractograms were evaluated using PANalytical High-Score software.

Potentiodynamic current/voltage ( $I/V$ ) sweeps were performed using a Keithley 6430 Subfemto-Remote-Source meter. A current compliance  $I_{CC}$  was adjusted between 10 nA and 50 μA to avoid high currents in the low resistive state (LRS) which destroys the cells. Different sweep rates ranging from 40 mV s<sup>-1</sup> to 3 V s<sup>-1</sup> were achieved by adjusting the voltage step size and time delay between each voltage step.

For a detailed analytical study of contact resistances the cells were switched ON by a voltage pulse with a current compliance of 100 nA. Subsequently, the current was increased by 100 nA per 2 s from 100 nA to 20 μA while simultaneously measuring the cell resistance.

Short pulses were accomplished using a Wavetek 100 MHz synthesized arbitrary waveform generator (model 395) and analyzed by a Tektronix TSD 684A digital oscilloscope. We reduced the cable length to measure signals with pulse lengths down to 50 ns. Therefore, the voltage signal was measured using a 50 Ω coupled input whereas a 1 MΩ

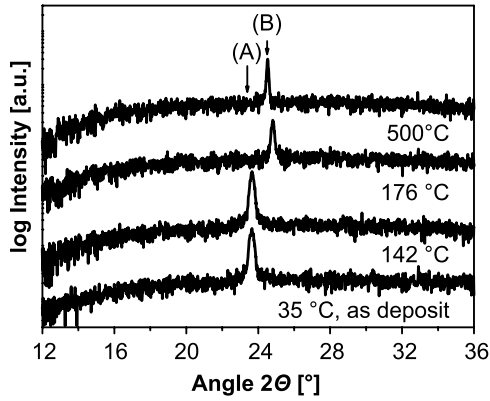


**Figure 2.** Crystalline responses measured by x-ray diffraction (XRD) while simultaneously heating the sample with  $4\text{ °C min}^{-1}$ . XRD peaks (A) and (B) correspond to the  $\gamma$ -AgI and  $\alpha$ -AgI phase, respectively.

coupled input in series to the cell was used to analyze the current response and decrease the current after switching to the LRS.

### 3. Results and discussion

All AgI films deposited in this study showed a pronounced crystalline  $\gamma$ -AgI structure at room temperature (figure 2) which is consistent with the results reported in the literature [19]. The reflection (A) at  $2\Theta = 23.62^\circ$  represents the  $\gamma$ -AgI phase, stable at temperatures below  $176\text{ °C}$ . Between  $142\text{ °C}$  and  $176\text{ °C}$  the peak (A) disappears and a new diffraction peak (B) at  $2\Theta = 24.78^\circ$  for  $176\text{ °C}$  and  $2\Theta = 24.48^\circ$  for  $500\text{ °C}$ , respectively, is formed, indicating the  $\gamma$ -AgI to  $\alpha$ -AgI transition [19]. The phase transition temperature corresponds to the reported literature value. We observed that the  $\alpha$ -AgI phase remains stable until AgI is melting above  $500\text{ °C}$ . The chemical stability of the AgI films was controlled by XRD measurements performed on as-deposited samples and samples being stored for three

months (protected from light) showing no change in the diffraction patterns.

For Ag/AgI/Pt microcrossbar cells we found that the thickness of the Ag layer compared to the AgI thickness is critical for the device functionality. If the Ag film thickness is in the range of a few tenths of nanometers (e.g. 30 nm) the electrode seems to chemically dissolve after the evaporation resulting in a high resistance of the cell. We are still unable to unequivocally identify the reason for this dissolution. However, impurities in silver iodide responsible for the Ag dissolution have not been found and the deposited films show x-ray diffraction (XRD) peaks of stoichiometric (poly-) crystalline AgI.

Typical resistive switching (RS) characteristics are shown in figure 3(a). Here, a current compliance  $I_{CC} = 100\text{ nA}$  is used to maintain the current in the low resistive ON state of the cell after switching at approximately  $V_{SET} = 80\text{ mV}$ . We found that Ag/AgI/Pt-based cells are showing a pronounced multilevel switching (figure 3(b)), whereas the ON resistance  $R_{ON}$  in the LRS can be controlled by variation of  $I_{CC}$ . As soon as the cell is switched to the ON state and the current compliance is reached the actual voltage applied to the cell decreases, i.e. the driving force for further filament growth becomes negligible. The almost purely electronic current then obeys Ohm's law resulting in a linear relation between  $R_{ON} \approx V_{SET}/I_{CC}$  [16]. The comparatively low SET voltage  $V_{SET}$  appears to be disadvantageous for particular memory applications because read voltages of less than 80 mV (e.g. 40 mV) are required to avoid resistive switching while reading the stored information of the cell. This can be avoided by the nonlinear switching kinetics which is discussed later in more detail.

After switching to the ON state, the actual applied cell voltage is regulated (lowered) by the Keithley 6430 source meter to adjust the preset current compliance (not depicted in figure 3(a)). This cell voltage differs from the programming voltage  $V_{Prog}$  in the range where the current compliance limits the total current and is characteristic for the filament resistance. Typical cell voltages during  $I/V$  sweep are shown in figure 4. We observed that, although the cell is

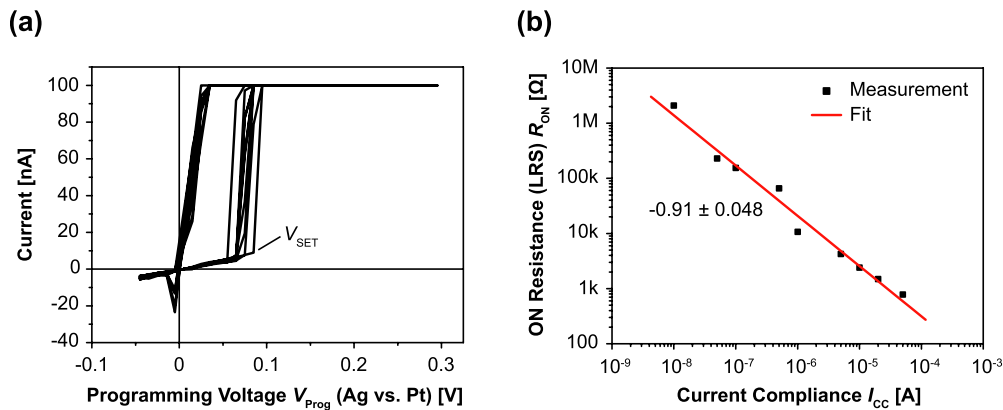


**Figure 3.** Resistive switching characteristics of Ag/AgI/Pt microcrossbars. (a) Typical switching behavior (current compliance  $I_{CC} = 100\text{ nA}$ ). (b) Multilevel switching: different ON resistances  $R_{ON}$  can be adjusted by variation of the current compliance.

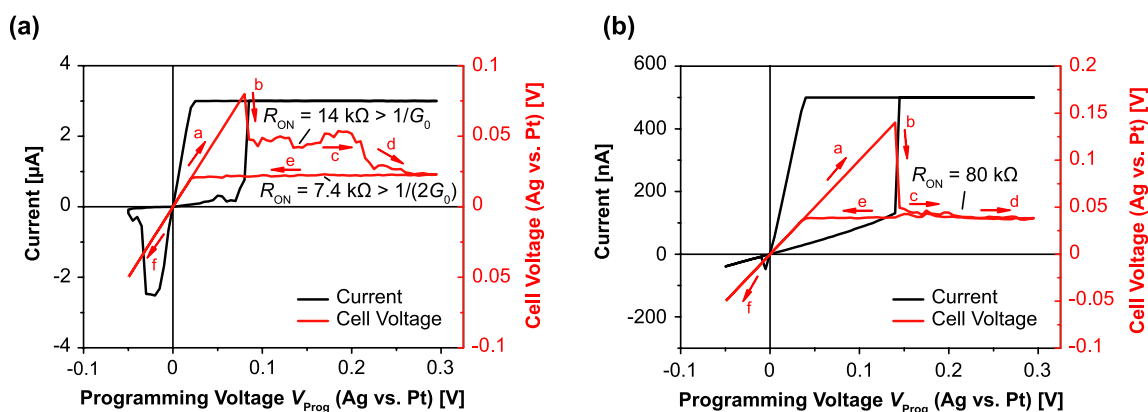


**Figure 4.** Analysis of filament formation by measuring the actual cell voltage drop simultaneously during  $I/V$  sweep. (a) Although the cell already switched, a significant voltage drop of about 25 mV is observed during further sweeping, indicating a quantized conductivity of the filament. (b) At lower current compliances a similar voltage drop is not observed. Red arrows (a)–(f) indicate the switching direction of the cell voltage.

switched to a specific ON resistance (depending on the current compliance), the actual cell voltage further decreases during the sweep (figure 4(a)). This can be understood in a further growth or strengthen of the metallic filament towards the WE since the driving force (cell voltage) for electrochemical filament formation is reduced but still effective. However, for comparatively high  $R_{ON} \gg 14 \text{ k}\Omega$  the voltage decrease is rather continuous or nearly not detectable which is shown in figure 4(b). It is remarkable, that only for low ON resistances  $R_{ON} < 14 \text{ k}\Omega$  a nearly discrete voltage drop is observed.

We attributed this to a different conductivity mechanism between the filament and the working electrode. In the case of high  $R_{ON}$  the overall conductivity of the cell seems to be dominated by tunneling between the filament and the WE [16]. By further growth of the filament the tunneling distance is reduced continuously, resulting in a gradual resistance change and hence gradual voltage drop. In contrast, in the case of  $R_{ON} < 14 \text{ k}\Omega$  the overall resistance is close to the resistance of a single atomic point contact  $R_0 = 1/G_0 = (2e^2/h)^{-1} \approx 12.9 \text{ k}\Omega \approx 1/(78 \mu\text{S})$  [20]. Hence, a single metal atom of the filament seems to be responsible for the conductivity mechanism. By further growth of the filament a second atom can contribute to the conductivity, resulting in a quantized decrease of the ON resistance and thus a discrete cell voltage drop. This could explain the discrete voltage steps in figure 4(a). However, in both cases the filament resistance  $R_f$  of about  $500 \Omega$ – $1 \text{ k}\Omega$  is in series either to the tunnel contact or the atomic point contact. A proposed equivalent circuit of the overall cell resistance is depicted in figure 5. The contact resistance  $R_c$ , the filament resistance  $R_f$  as well as the resistance of the Ag and Pt electrodes  $R_e$  are contributing to the total cell resistance  $R_{ON}$  in the ON state. Note  $R_f$  and  $R_c$  may vary during measurement and depend on the cell voltage due to further filament growth whereas  $R_e \ll 100 \Omega$  depends only on the device geometry and conductivity of Ag and Pt and will be further neglected for simplification.

We observed quantized resistances only within a current window of  $1$ – $10 \mu\text{A}$ . By conventional  $I/V$  sweeps (figure 4(a)) we were not able to detect more than one or two

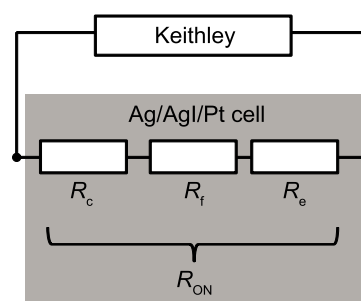


**Figure 5.** Equivalent circuit for a simple measurement set-up consisting of the Ag/AgI/Pt cell and the Keithley source meter. The electrode resistance  $R_e$  is small compared to the contact resistance  $R_c$  and the filament resistance  $R_f$ . Hence,  $R_e$  will be further neglected.

discrete voltage drops. Alternatively, more discrete resistance levels can be achieved by a current sweep measurement as shown in figure 6(a). At the beginning the cell is switched ON with a current compliance of  $100 \text{ nA}$ . Subsequently, the current is increased stepwise from  $100 \text{ nA}$  to  $20 \mu\text{A}$  by  $100 \text{ nA}$  and  $2 \text{ s}$  per step. The cell resistance was simultaneously measured. In figure 6(a) at least five quantized resistances can be observed which fitted well to integer multiple of the conductivity  $G_0$  of a one atomic point contact. Here, a filament resistance  $R_f = 800 \Omega$  was assumed. Note, the current resulting in specific resistance steps varies from cell to cell and some multiples (e.g.  $1G_0$  or  $5G_0$  in this example) seemed to be skipped during measurement.

Due to the statistical variation from cell to cell 65 cells have been measured resulting in a total number of more than 20 000 conductivity measurement points. Based on these measurement points a cumulative statistics of the cell conductivity has been calculated. Therefore, we assume  $R_f = 800 \Omega$  which fits well to the resistance calculated by the literature value of the conductivity of Ag, a length of  $30 \text{ nm}$  and a diameter of  $1$ – $2 \text{ nm}$  [16]. The result is shown in figure 6(b). It is remarkable that maximum of the cumulative probability for specific conductivities  $nG_0$  (with

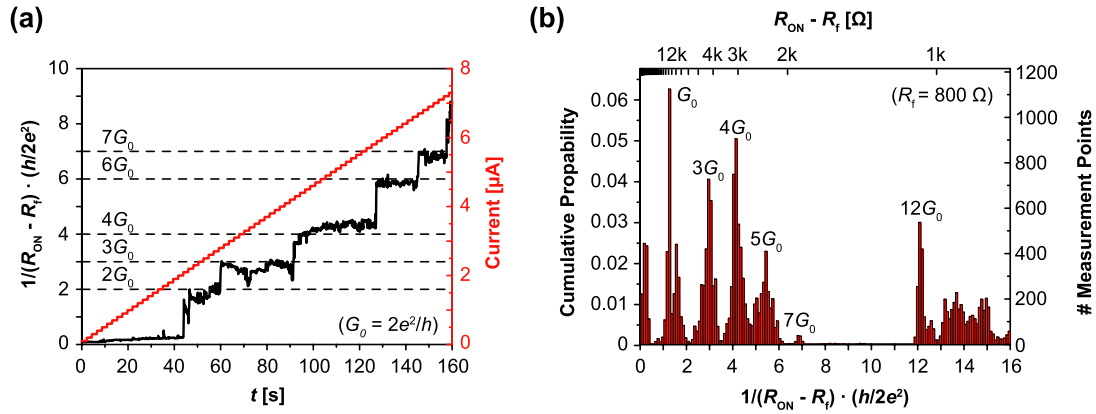


**Figure 6.** Analysis of quantized cell conductance by a current sweep. (a) At least five quantized resistances have been observed in this example by current sweeping. (b) Cumulative statistics of measured cell conductivity.

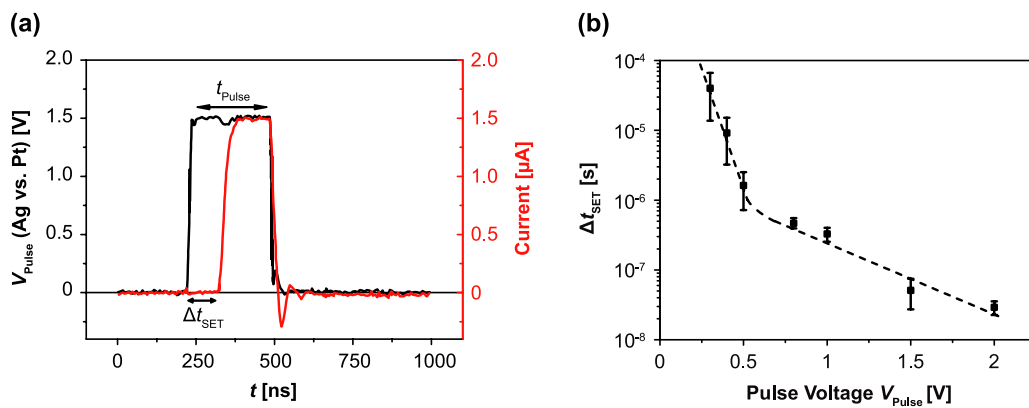


**Figure 7.** Analysis of the kinetics of Ag/AgI/Pt microcrossbars. (a) Short pulse measurement with definition of  $\Delta t_{\text{SET}}$  exemplary for pulse amplitude of 1.5 V and a pulse length of  $t_{\text{Pulse}} = 250$  ns. (b) Switching kinetics for pulse measurement. At high pulse amplitudes  $V_{\text{Pulse}}$  the switching time can be decreased down to 10 ns and below.

$n = 1, 2, 3, \dots$ ) are observed. In particular, the maxima for  $n = 1, 3, 4, 5$  are distinctive. Variation of the actual filament resistance from cell to cell and during measurement may result in deviation from the exact conductivity  $nG_0$ . The reason for the gap between  $7G_0$  and  $12G_0$  is yet unclear. It was found that below a cell resistance of about 2 k $\Omega$  the cell resistance drops fast below 1 k $\Omega$ . Hence, it is assumed that the measurement is too slow to detect resistances between 2 and 1 k $\Omega$ . Thus, in a cumulative statistics these resistances are not contributing. Below 1 k $\Omega$  the cell resistance is nearly constant and may be dominated by the filament resistance. Therefore, this resistance is again contributing to the cumulative statistics.

To analyze the switching kinetics we varied the sweep rate between 40 mV s $^{-1}$  and 3 V s $^{-1}$  for potentiodynamic measurements. Within this range  $V_{\text{SET}} \approx 0.085$  V was found to be nearly independent of the sweep rate. However, a strong exponential relation between the pulse amplitude  $V_{\text{Pulse}}$  and the switching time  $\Delta t_{\text{SET}}$  is observed for short pulse measurements when applying voltage pulses above 0.5 V. This has been demonstrated for various resistive switching materials as well [2, 3]. A typical voltage pulse and the current response of the cell are depicted in figure 7(a). Here, the pulse length is  $t_{\text{Pulse}} = 250$  ns with an applied voltage of  $V_{\text{Pulse}} = 1.5$  V. The switching time  $\Delta t_{\text{SET}}$  is defined as the

time shift between the voltage signal rise and the current signal rise. We reduced cable lengths and performed short circuit measurements to ensure that the delay between voltage and current signal is not dominated by the measurement set-up. The current was reduced by a series resistor using the 1 M $\Omega$  input resistance of the oscilloscope which is also acting as the signal source for the current. The switching kinetics is shown in figure 7(b). Between  $V_{\text{Pulse}} = 0.25$  and 2 V the switching time  $\Delta t_{\text{SET}}$  is decreased by more than three orders of magnitude. We observed fast switching within at least 10 ns at moderate switching voltages below 2 V. Note that below  $V_{\text{Pulse}} = 0.5$  V the switching time increases by decrease of the pulse amplitude and seems to asymptotically approach a threshold value. This threshold value could be the reason for the constant switching voltage observed by variation of the sweep rate for potentiodynamic measurements.

As shown in figure 3(a) the cell is switching at a low voltage (80 mV) for quasi-static measurement conditions, which is disadvantageous for memory applications since it drastically reduces the read voltage margin. However, fast read and write pulses are preferably required for memory applications. According to the nonlinear switching kinetics the read voltage margin can be significantly increased for short read pulses (e.g.  $V_{\text{Read}} = 1$  V and  $t_{\text{Read}} = 50$  ns) to

avoid unintended switching of the cell. This concept has been recently approved for a nondestructive readout of ECM-based complementary resistive switches (CRS) [21] which show similar switching kinetics.

The origin of the nonlinear switching kinetics and especially for the threshold value for the switching is conflictingly discussed in the literature. For the Cu/SiO<sub>2</sub>/Pt ECM system it has been assumed that the electrocrystallization of the mobile metal ions at the counter electrode is rate-limiting [12]. This involves the nucleation rate of the metal ion at the cathode as well as the charge transfer at the anode/electrolyte interface. In particular, the threshold voltage for the Cu/SiO<sub>2</sub>/Pt system is contributed to the nucleation overpotential of the metal ions at the counter electrode [12]. We assume this situation holds for AgI thin films as well.

#### 4. Summary

In this work we presented a fabrication approach for AgI-based resistively switching microcrossbar structured ECM cells. We investigated the switching behavior and reported on a pronounced multilevel switching which offers the potential of multibit storage. By measuring the cell resistance during  $I/V$  sweep we observed that the ON resistance is decreasing during measurement potentially due to further strengthening of the filament. For  $R_{ON} < 14$  k $\Omega$  discrete resistance changes can be observed, indicating a single atomic point contact for the ON state whereas for  $R_{ON} > 14$  k $\Omega$  the resistance of the cell seems to be dominated by tunneling between the filament and the working electrode. We were able to measure at least five quantized resistance levels by current sweeping which are further supported by cumulative statistics. According to the switching kinetics we found a strong nonlinearity of the switching time and the voltage pulse amplitude. Switching within at least 10 ns at moderate voltages at 2 V has been proved, making this system of potential interest for fast switching memory devices.

#### Acknowledgments

The authors would like to thank P Roegels for preparing the thermal evaporation of AgI thin films and S Menzel for fruitful discussions. This work was supported in parts by the Samsung Global Research Outreach Program.

#### References

- [1] Waser R and Aono M 2007 Nanoionics-based resistive switching memories *Nature Mater.* **6** 833–40
- [2] Waser R, Dittmann R, Staikov G and Szot K 2009 Redox-based resistive switching memories—nanoionic mechanisms, prospects, and challenges *Adv. Mater.* **21** 2632–63
- [3] Valov I, Waser R, Jameson J R and Kozicki M N 2011 Electrochemical metallization memories—fundamentals, applications, prospects *Nanotechnology* **22** 254003
- [4] Schindler C, Weides M, Kozicki M N and Waser R 2008 Low current resistive switching in Cu–SiO<sub>2</sub> cells *Appl. Phys. Lett.* **92** 122910
- [5] Yang L, Kügeler C, Szot K, Rüdiger A and Waser R 2009 The influence of copper top electrodes on the resistive switching effect in TiO<sub>2</sub> thin films studied by conductive atomic force microscopy *Appl. Phys. Lett.* **95** 13109
- [6] Sakamoto T, Lister K, Banno N, Hasegawa T, Terabe K and Aono M 2007 Electronic transport in Ta<sub>2</sub>O<sub>5</sub> resistive switch *Appl. Phys. Lett.* **91** 92110
- [7] Kozicki M N 2007 Memory devices based on solid electrolytes *Mater. Res. Soc. Symp. Proc.* **997** 165–74
- [8] Kozicki M N, Balakrishnan M, Gopalan C, Ratnakumar C and Mitkova M 2006 Programmable metallization cell memory based on Ag–Ge–S and Cu–Ge–S solid electrolytes *Proc. Non-Volatile Memory Technology Symp.* pp 83–9
- [9] Schindler C, Guo X, Besmehn A and Waser R 2007 Resistive switching in Ge<sub>0.3</sub>Se<sub>0.7</sub> films by means of copper ion migration *Int. J. Res. Phys. Chem. Chem. Phys.* **221** 1469–78
- [10] Tappertzhofen S, Menzel S, Valov I and Waser R 2011 Redox processes in silicon dioxide thin films using copper microelectrodes *Appl. Phys. Lett.* **99** 203103
- [11] Schindler C, Thermadam S C P, Waser R and Kozicki M N 2007 Bipolar and unipolar resistive switching in Cu-doped SiO<sub>2</sub> *IEEE Trans. Electron Devices* **54** 2762–8
- [12] Schindler C, Staikov G and Waser R 2009 Electrode kinetics of Cu–SiO<sub>2</sub>-based resistive switching cells: overcoming the voltage–time dilemma of electrochemical metallization memories *Appl. Phys. Lett.* **94** 072109
- [13] Liang X F, Chen Y, Shi L, Lin J, Yin J and Liu Z G 2007 Resistive switching and memory effects of AgI thin film *J. Phys. D: Appl. Phys.* **40** 4767–70
- [14] Tatsumisago M, Okuda K, Itakura N and Minami T 1999 Crystallization of  $\alpha$ -AgI from AgI–Ag<sub>2</sub>O–M<sub>x</sub>O<sub>y</sub> (M<sub>x</sub>O<sub>y</sub> = B<sub>2</sub>O<sub>3</sub>, GeO<sub>2</sub>, WO<sub>3</sub>) melts and glasses *Solid State Ion.* **121** 193–200
- [15] Guo H X, Yang B, Chen L, Xia Y D, Yin K B, Liu Z G and Yin J 2007 Resistive switching devices based on nanocrystalline solid electrolyte (AgI)<sub>0.5</sub>(AgPO<sub>3</sub>)<sub>0.5</sub> *Appl. Phys. Lett.* **91** 243513
- [16] Menzel S, Böttger U and Waser R 2012 Simulation of multilevel switching in electrochemical metallization memory cells *J. Appl. Phys.* **111** 014501
- [17] Terabe K, Hasegawa T, Nakayama T and Aono M 2005 Quantized conductance atomic switch *Nature* **433** 47–50
- [18] Nayak A, Tsuruoka T, Terabe K, Hasegawa T and Aono M 2011 Switching kinetics of a Cu<sub>2</sub>S-based gap-type atomic switch *Nanotechnology* **22** 235201
- [19] Kondo S, Itoh T and Saito T 1998 Strongly enhanced optical absorption in quench-deposited amorphous AgI films *Phys. Rev. B* **57** 13235–40
- [20] Krans J, Muller C, Yanson I, Govaert T, Hesper R and van Ruitenbeek J M 1993 One-atom point contacts *Phys. Rev. B* **48** 14721–4
- [21] Tappertzhofen S, Linn E, Nielen L, Rosezin R, Lentz F, Bruchhaus R, Valov I, Böttger U and Waser R 2011 Capacity based nondestructive readout for complementary resistive switches *Nanotechnology* **22** 395203